

# Nickel-Catalyzed Copolymerization of Ethylene and Vinyltrialkoxysilanes: Catalytic Production of Cross-Linkable Polyethylene and Elucidation of the Chain-Growth Mechanism

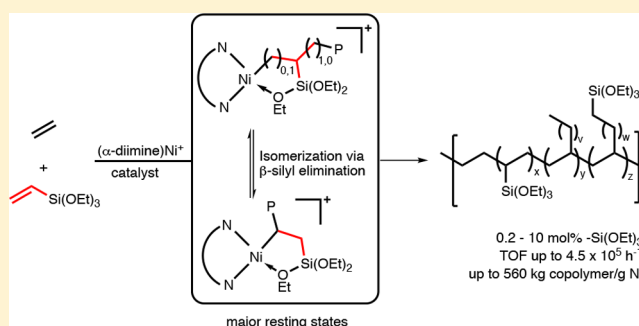
Zhou Chen,<sup>†</sup> Mark D. Leatherman,<sup>‡</sup> Olafs Daugulis,<sup>\*,†</sup> and Maurice Brookhart<sup>\*,†,‡</sup>

<sup>†</sup>Center for Polymer Chemistry, Department of Chemistry, University of Houston, Houston, Texas 77204-5003, United States

<sup>‡</sup>Department of Chemistry, University of North Carolina at Chapel Hill, Chapel Hill, North Carolina 27599-3290, United States

## Supporting Information

**ABSTRACT:** Copolymerizations of ethylene with vinyltrialkoxysilanes using cationic ( $\alpha$ -diimine)Ni(Me)(CH<sub>3</sub>CN)<sup>+</sup> complexes **4a,b**/B(C<sub>6</sub>F<sub>5</sub>)<sub>3</sub> yield high molecular weight copolymers exhibiting highly branched to nearly linear backbones depending on reaction conditions and catalyst choice. Polymerizations are first-order in ethylene pressure and inverse-order in silane concentration. Microstructural analysis of the copolymers reveals both in-chain and chain-end incorporation of -Si(OR)<sub>3</sub> groups whose ratios depend on temperature and ethylene pressure. Detailed low-temperature NMR spectroscopic investigations show that well-defined complex **3b** ( $\alpha$ -diimine)Ni(Me)(OEt<sub>2</sub>)<sup>+</sup> reacts rapidly at -60 °C with vinyltrialkoxysilanes via both 2,1 and 1,2 insertion pathways to yield 4- and 5-membered chelates, respectively. Such chelates are the major catalyst resting states but are in rapid equilibrium with ethylene-opened chelates, ( $\alpha$ -diimine)Ni(R)-(C<sub>2</sub>H<sub>4</sub>)<sup>+</sup> complexes, the species responsible for chain growth. Chelate rearrangement via  $\beta$ -silyl elimination accounts for formation of chain-end -Si(OR)<sub>3</sub> groups and constitutes a chain-transfer mechanism. Chelate formation and coordination of the Ni center to the ether moiety, R-O-Si, of the vinylsilane somewhat decreases the turnover frequency (TOF) relative to ethylene homopolymerization, but still remarkably high TOFs of up to  $4.5 \times 10^5 \text{ h}^{-1}$  and overall productivities can be achieved. Activation of readily available ( $\alpha$ -diimine)NiBr<sub>2</sub> complexes **2** with a combination of AlMe<sub>3</sub>/B(C<sub>6</sub>F<sub>5</sub>)<sub>3</sub>/[Ph<sub>3</sub>C][B(C<sub>6</sub>F<sub>5</sub>)<sub>4</sub>] yields a highly active and productive catalyst system for the convenient synthesis of the copolymer, a cross-linkable PE. For example, copolymers containing 0.23 mol % silane can be generated at 60 °C, 600 psig ethylene over 4 h with a productivity of 560 kg copolymer/g Ni. This method offers an alternative route to these materials, normally prepared via radical routes, which are precursors to the commercial cross-linked polyethylene, PEX-b.



## INTRODUCTION

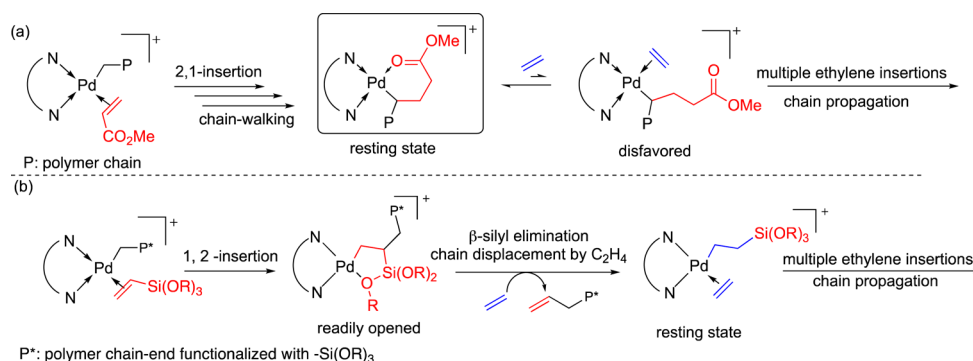
The study of late metal-catalyzed olefin polymerizations has advanced substantially in recent years.<sup>1</sup> A primary motivating factor for the development of late-metal catalysts is that their less oxophilic nature, in comparison with early metal catalysts, renders them more compatible with polar monomers. Of particular interest is the copolymerization of ethylene and readily available, inexpensive polar vinyl monomers.<sup>2</sup> An early report from our group showed that cationic  $\alpha$ -diimine Pd(II) complexes copolymerize ethylene and methyl acrylate (MA) to form highly branched copolymers in which acrylate is preferentially incorporated at chain ends.<sup>3</sup> Mechanistic studies revealed that a six-membered carbonyl chelate intermediate was formed following 2,1 insertion of MA and rapid chain-walking (Scheme 1a).<sup>4</sup> This chelate, the catalyst resting state, is highly favored over the “chelate-opened” ethylene complex required for further chain growth.

An extensive family of neutral Pd(II) catalysts based on phosphine-sulfonate ligands (“Drent-type” catalysts)<sup>5</sup> and

cationic Pd(II) catalysts derived from bisphosphine monoxide type ligands have been developed for ethylene homo- and copolymerizations.<sup>6</sup> Many of these systems successfully copolymerize ethylene with a variety of vinyl polar monomers including methyl acrylate,<sup>7</sup> vinyl acetate,<sup>8</sup> vinyl fluoride,<sup>9</sup> acrylonitrile,<sup>10</sup> vinyl ethers,<sup>11</sup> and other important polar monomers.<sup>12</sup> In contrast to the palladium  $\alpha$ -diimine systems, linear functionalized polyethylenes are obtained. Activities of these systems in copolymerizations are invariably substantially less than for ethylene homopolymerizations, and low molecular weight copolymers are generally produced.

Nickel(II) analogues supported by  $\alpha$ -diimine,<sup>13</sup> phosphine-sulfonate,<sup>14</sup> and bisphosphine monoxide ligands<sup>6c</sup> noted above have received limited attention for ethylene/polar vinyl monomer copolymerizations. While these systems generally exhibit much higher activities for homopolymerization of

Received: September 26, 2017

Scheme 1. Proposed Mechanism of  $\alpha$ -Diimine Pd(II)-Catalyzed Copolymerization of Ethylene with (a) MA and (b) Vinyltrialkoxysilane

ethylene relative to Pd analogues, copolymerizations that have been examined generally show strong rate retardation or complete suppression by the polar functional group.<sup>15–17</sup> The development of practical catalysts for ethylene/polar vinyl monomer copolymerizations which exhibit commercially viable activities, productivities, and molecular weights remains a continuing challenge for this field.

Polyethylene that is functionalized with trialkoxysilane ( $-\text{Si}(\text{OR})_3$ ) groups can be cross linked to form PEX-b, a tough material that is widely used for power cable insulation and hot water piping systems.<sup>18</sup> This cross-linkable polymer is produced commercially either by radical-induced grafting of vinyl silanes to polyethylene (PE) or radical-initiated copolymerization of ethylene and the vinyl silane, a process requiring exceptionally high pressures and temperatures. Since only low levels of  $-\text{Si}(\text{OR})_3$  are required for cross-linking (ca. 0.1–2.0 mol %),<sup>19</sup> metal-catalyzed copolymerization of ethylene and vinyltrialkoxysilanes provides a potentially viable alternative method for the synthesis of this modified PE.<sup>16b,20</sup> Recently, we reported mechanistic studies following up a DuPont patent disclosure<sup>20a</sup> that  $\alpha$ -diimine Pd(II) complexes catalyze copolymerization of ethylene and vinyltriethoxysilane to yield low molecular weight polymers/oligomers.<sup>20b,21</sup> We showed that copolymerizations proceed at rates comparable to ethylene homopolymerization since the catalyst resting state is an alkyl ethylene complex. The turnover frequency is independent of ethylene pressure and is controlled by the rate of migratory insertion. Low-temperature NMR studies revealed that a silyl ether chelate intermediate is formed after 1,2 insertion of vinyltrialkoxysilane, but this chelate is rapidly and completely opened with ethylene. Thus, unlike the methyl acrylate system, formation of the chelate does not retard copolymerization rates (Scheme 1b). The chelate undergoes facile  $\beta$ -silyl elimination and displacement of the unsaturated chain by ethylene, resulting in chain transfer and formation of low molecular weight copolymers exhibiting chain-end incorporation of vinyltrialkoxysilane.<sup>21</sup>

Due to the high cost of palladium and the relatively low activities and lifetimes of these Pd(II) catalysts, Pd-catalyzed copolymerizations hold little commercial interest. In the same patent disclosure, the DuPont group reported extensive screening of nickel  $\alpha$ -diimine catalysts for copolymerization of ethylene and vinyltrialkoxysilanes.<sup>20a</sup> The most active catalysts as shown in eq 1 were generated via activation of the bis-trimethylsilyl-functionalized Ni complex **1** at 60 °C with a combination of  $\text{B}(\text{C}_6\text{F}_5)_3$  and  $\text{LiB}(\text{C}_6\text{F}_5)_4$ .

In this paper, we report a comprehensive synthetic and mechanistic investigation of this copolymerization reaction employing well-defined cationic nickel  $\alpha$ -diimine catalysts. A combination of bulk copolymerization data, low-temperature NMR characterizations of intermediates and their reactivities, and the analysis of copolymer molecular weights and microstructures provide a complete profile of the chain growth process, including identification of the catalyst resting states, the mode of insertion of the vinylsilanes, the dependence of the turnover frequency on ethylene and vinylsilane concentrations, and the role of chelate intermediates and their isomerization reactions in determining the polymer enchainment modes of the vinylsilanes. Furthermore, we report a simple method for activating readily available  $\alpha$ -diimine nickel dibromide complexes **2** (Figure 1),

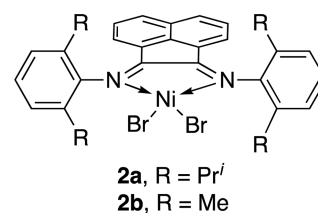
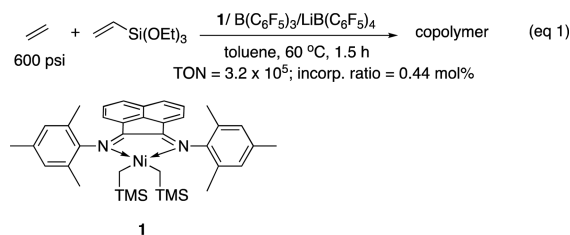


Figure 1.  $\alpha$ -Diimine nickel dibromide complexes **2**.

which allows convenient synthesis of high molecular weight copolymers with productivities of up to 560 kg copolymer/g Ni at 60 °C over 4 h with 0.23 mol % incorporation of silane.

## RESULTS

**Copolymerization Reactions.** The well-defined nickel catalysts employed here for the mechanistic studies of the copolymerization reactions are the cationic  $\alpha$ -diimine nickel methyl ether complexes **3a,b** and the nickel methyl acetonitrile complexes **4a,b**, which were readily synthesized from nickel ether complexes **3a,b** (Figure 2; see the SI for details).<sup>22</sup> Catalysts **4a,b**<sup>23</sup> are activated with  $\text{B}(\text{C}_6\text{F}_5)_3$ , which abstracts the nitrile ligand. They show activities in ethylene homopolymerization



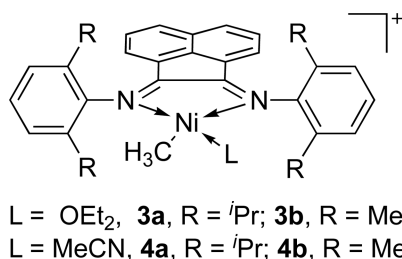


Figure 2. Well-defined  $\alpha$ -diimine Ni(II) complexes **3** and **4**.

similar to those of typical ( $\alpha$ -diimine)NiBr<sub>2</sub> catalysts **2a,b** activated with modified methylaluminoxane (MMAO) (see SI). Vinyltriethoxysilane (VTEoS) was chosen as a model CH<sub>2</sub>=CHSi(OR)<sub>3</sub> monomer.

#### Investigation of Tetraisopropyl-Substituted Complex

**4a.** Results of copolymerizations of ethylene and VTEoS using **4a**/B(C<sub>6</sub>F<sub>5</sub>)<sub>3</sub> are summarized in Table 1. Highly branched polymers are formed from **4a**/B(C<sub>6</sub>F<sub>5</sub>)<sub>3</sub> via the well-established chain-running mechanism<sup>24</sup> with branching densities ranging from ca. 25–95 branches per 1000 carbons depending on reaction conditions. Copolymerization temperatures were screened from 40 to 100 °C at 200 psig pressure of ethylene (entries 1–4). Branching densities and the mole fraction incorporation of VTEoS into the polymer increase as temperature increases with a corresponding decrease in *M<sub>n</sub>*. (The increase in silane incorporation with increasing temperature is likely primarily due to decreasing solubility of ethylene at higher temperatures.)<sup>25</sup> For example, at 40 °C, 0.37 mol % incorporation of silane is obtained with 22 br/1000 C and a *M<sub>n</sub>* of 173 kg/mol, while at 100 °C, 0.93 mol % incorporation of silane is achieved in the polymer, with a high branching density of 94 br/1000 C and a lower *M<sub>n</sub>* of 27 kg/mol. It is well-known that  $\alpha$ -diimine nickel catalysts decompose rapidly in ethylene homopolymerizations at temperatures above ca. 60 °C.<sup>26,27</sup> Interestingly, the turnover frequency (TOF) of copolymerization (0.5 h runs) decreases only slightly from 5.3 × 10<sup>4</sup> h<sup>-1</sup> at 60 °C to 4.1 × 10<sup>4</sup> h<sup>-1</sup> at 80 °C. Moreover, **4a**/B(C<sub>6</sub>F<sub>5</sub>)<sub>3</sub> exhibits fairly constant copolymerization activity over 1 h at 60 °C (compare TOF entry 2, 30 min to TOF entry 5, 60 min). These results suggest that this catalyst exhibits better thermal stability under copolymerization conditions relative to homopolymerization conditions.

Copolymerizations were then carried out at 60 °C for 30 min under various ethylene pressures and concentrations of VTEoS (entries 2 and 6–11). As expected, at a fixed ethylene pressure, the incorporation of VTEoS into the copolymer is nearly proportional to the VTEoS concentration. At the same time, the TOF is inversely proportional to the concentration of VTEoS (compare entries 2, 6, 7 and entries 9–11). Likewise, at a given VTEoS concentration, the TOF increases proportionally to the ethylene pressure (compare entries 6, 8, 10). Plots illustrating these dependencies are shown in the SI. The fact that the TOFs in these copolymerizations are essentially first-order in ethylene shows that the catalyst resting state is *not* a nickel alkyl ethylene complex in contrast to the analogous palladium systems.<sup>20b</sup> As expected from homopolymerization studies, increasing ethylene pressure results in decreasing branching densities due to more rapid trapping and insertion relative to chain-walking.<sup>24b</sup> Notably, complex **4a** exhibits a TOF of 2.0 × 10<sup>4</sup> h<sup>-1</sup>, reduced by a only factor of 7 in absence of activator B(C<sub>6</sub>F<sub>5</sub>)<sub>3</sub> (entries 9 vs 12).

We wished to examine the potential role of coordination of the Si–O–R ether linkage to the Ni center with respect to competition with ethylene and retardation of the turnover frequency. Si(OEt)<sub>4</sub>, which lacks a reactive vinyl group, was used as a model for vinyltriethoxysilane. Table 2 summarizes several control experiments. The homopolymerization of ethylene (200 psig, 60 °C, 30 min) by **4a**/B(C<sub>6</sub>F<sub>5</sub>)<sub>3</sub> is retarded by a factor of ca. 2 when carried out in the presence of 0.5 M Si(OEt)<sub>4</sub> (entries 1 vs 2), which indicates that the silyl ether groups of Si(OEt)<sub>4</sub> effectively compete with ethylene for binding to the Ni center, and a major resting state under these conditions is an ( $\alpha$ -diimine)Ni(R)[Si( $\kappa$ -OEt)(OEt)<sub>3</sub>]<sup>+</sup> species. When the copolymerization using 0.5 M VTEoS is compared to the homopolymerization, the suppression factor, 4*X*, is greater than for Si(OEt)<sub>4</sub> (entries 1 vs 3), suggesting a Ni ether complex ( $\alpha$ -diimine)Ni(R)[Si( $\kappa$ -OEt)(OEt)<sub>2</sub>(CHCH<sub>2</sub>)]<sup>+</sup> may play a role in retarding the rate of copolymerization relative to homopolymerization, but this is likely not the only factor involved. This is further confirmed by comparing entry 3 with a copolymerization run using 0.5 M VTEoS and an additional 0.5 M Si(OEt)<sub>4</sub> (entry 4). The added 0.5 M Si(OEt)<sub>4</sub> further suppresses the rate by a factor of 2.5, implying that the Ni complex in the copolymerization in entry 3 cannot be completely tied up as an ether complex; otherwise, no additional rate suppression would have been observed on addition of Si(OEt)<sub>4</sub>.

Table 1. Copolymerizations Using ( $\alpha$ -Diimine)Ni(Me)(MeCN)<sup>+</sup> Catalyst **4a**/B(C<sub>6</sub>F<sub>5</sub>)<sub>3</sub><sup>a</sup>

entry	<i>T</i> (°C)	C <sub>2</sub> H <sub>4</sub> (psig)	[VTEoS] (M)	yield (g)	TOF (× 10 <sup>-4</sup> h <sup>-1</sup> )	branches/1000 C <sup>b</sup>	<i>M<sub>n</sub></i> <sup>c</sup> (kg/mol)	<i>M<sub>w</sub></i> / <i>M<sub>n</sub></i> <sup>c</sup>	incorp <sup>b</sup> (mol %)	<i>T<sub>m</sub></i> <sup>d</sup> (°C)
1	40	200	0.5	1.0	4.8	22	173	1.4	0.37	99
2	60	200	0.5	1.1	5.3	50	104	1.6	0.69	64
3	80	200	0.5	0.85	4.1	73	62	1.8	0.79	22
4	100	200	0.5	0.13	0.6	94	27	1.6	0.93	-29
5 <sup>e</sup>	60	200	0.5	1.9	4.5	51	106	1.9	0.68	66
6	60	200	1.0	0.56	2.7	51	85	1.7	1.30	57
7	60	200	1.5	0.29	1.4	49	61	1.7	2.20	57
8	60	400	1.0	1.0	4.8	40	112	1.5	0.72	78
9	60	600	0.5	2.9	14	34	138	1.4	0.23	89
10	60	600	1.0	1.4	6.8	32	128	1.4	0.46	89
11	60	600	1.5	0.92	4.4	34	110	1.5	0.72	85
12 <sup>f</sup>	60	600	0.5	0.41	2.0	36	84	1.8	0.24	87

<sup>a</sup>V(total) = 50 mL, 1.5 μmol of **4a**, 10 equiv of B(C<sub>6</sub>F<sub>5</sub>)<sub>3</sub>, 30 min, toluene solvent. <sup>b</sup>Determined by using <sup>1</sup>H NMR spectroscopy. <sup>c</sup>*M<sub>n</sub>* and *M<sub>w</sub>*/*M<sub>n</sub>* were determined by SEC in trichlorobenzene at 150 °C. <sup>d</sup>Determined by differential scanning calorimetry, second heating. <sup>e</sup>60 min. <sup>f</sup>No B(C<sub>6</sub>F<sub>5</sub>)<sub>3</sub>.

**Table 2. Control Polymerizations Using ( $\alpha$ -Diimine)Ni(Me)(MeCN)<sup>+</sup> Catalyst **4a**/B(C<sub>6</sub>F<sub>5</sub>)<sub>3</sub><sup>a</sup>**

entry	monomer [0.5 M]	additive [0.5 M]	yield (g)	TOF ( $\times 10^{-4}$ h <sup>-1</sup> )	branches/1000 C <sup>b</sup>	M <sub>n</sub> <sup>c</sup> (kg/mol)	M <sub>w</sub> /M <sub>n</sub> <sup>c</sup>	incorp. <sup>b</sup> (mol %)	T <sub>m</sub> <sup>d</sup> (°C)
1			4.5	22	54	125	1.6		48
2		Si(OEt) <sub>4</sub>	2.6	13	57	126	1.6		59
3	VTEoS		1.1	5.3	50	104	1.6	0.69	64
4	VTEoS	Si(OEt) <sub>4</sub>	0.42	2.0	53	90	1.6	0.71	63
5 <sup>e</sup>			3.0	43	60	135	1.7		55
6 <sup>e</sup>		Si(OEt) <sub>4</sub>	1.7	25	53	112	1.7		60

<sup>a</sup>V(total) = 50 mL, 1.5  $\mu$ mol of **4a**, 10 equiv of B(C<sub>6</sub>F<sub>5</sub>)<sub>3</sub>, 30 min, 60 °C, 200 psig C<sub>2</sub>H<sub>4</sub>, toluene solvent. <sup>b</sup>Determined by using <sup>1</sup>H NMR spectroscopy. <sup>c</sup>M<sub>n</sub> and M<sub>w</sub>/M<sub>n</sub> were determined by SEC in trichlorobenzene at 150 °C. <sup>d</sup>Determined by differential scanning calorimetry, second heating. <sup>e</sup>10 min.

**Table 3. Copolymerizations Using ( $\alpha$ -Diimine)Ni(Me)(MeCN)<sup>+</sup> Catalyst **4b**/B(C<sub>6</sub>F<sub>5</sub>)<sub>3</sub><sup>a</sup>**

entry	C <sub>2</sub> H <sub>4</sub> (psig)	[VTEoS] (M)	yield (g)	TOF ( $\times 10^{-4}$ h <sup>-1</sup> )	branches/1000 C <sup>b</sup>	M <sub>n</sub> <sup>c</sup> (kg/mol)	M <sub>w</sub> /M <sub>n</sub> <sup>c</sup>	incorp <sup>b</sup> (mol %)	ratio <sup>b</sup> (x/z)	T <sub>m</sub> <sup>d</sup> (°C)
1	200	0.5	3.4	4.1	16	14	2.2	3.0	1.0/1.9	95
2 <sup>e</sup>	200	0.5	6.3	3.8	16	14	2.1	3.1	1.0/1.9	95
3 <sup>f</sup>	200	1.5	2.4	1.2	14	8.8	1.6	8.5	1.0/1.9	48
4 <sup>f,g</sup>	200	1.5	1.6	0.8	29	6.9	1.5	10	1.0/2.8	17
5	600	1.5	3.8	4.6	9	14	2.0	3.2	1.0/1.1	97
6 <sup>h</sup>	600	0.5	6.1	14.5	9	23	2.0	1.0	1.0/1.1	115
7 <sup>h,i</sup>	600	0.1	19	45	10	29	2.1	0.23	n.d. <sup>j</sup>	115
8 <sup>i,k</sup>	600	0	6.2	177	5	85	2.2			135

<sup>a</sup>V(total) = 50 mL, 6.0  $\mu$ mol of **4b**, 10 equiv of B(C<sub>6</sub>F<sub>5</sub>)<sub>3</sub>, 30 min, 60 °C, toluene solvent. <sup>b</sup>Determined by using <sup>1</sup>H NMR spectroscopy. <sup>c</sup>M<sub>n</sub> and M<sub>w</sub>/M<sub>n</sub> were determined by SEC in trichlorobenzene at 150 °C. <sup>d</sup>Determined by differential scanning calorimetry, second heating. <sup>e</sup>60 min. <sup>f</sup>15  $\mu$ mol of **4b**. <sup>g</sup>80 °C. <sup>h</sup>3  $\mu$ mol of **4b**, 20 equiv of B(C<sub>6</sub>F<sub>5</sub>)<sub>3</sub>. <sup>i</sup>V(total) = 200 mL. <sup>j</sup>Not determined due to low VTEoS incorporation. <sup>k</sup>1.5  $\mu$ mol of **4b**, 20 equiv of B(C<sub>6</sub>F<sub>5</sub>)<sub>3</sub>, 35 °C, 5 min.

(mechanistic studies below will clarify the nature of the catalyst resting states). In contrast to the enhanced lifetime of the copolymerization, the decrease in activity of homopolymerization with time in the presence of Si(OEt)<sub>4</sub> at 60 °C is similar to that of the homopolymerization with no additive (compare entries 2 vs 6 with entries 1 vs 5, Table 2).

Very low molecular weight copolymers are produced by the analogous Pd complexes,<sup>20b,21</sup> while much higher molecular weight copolymers are generated by **4a**/B(C<sub>6</sub>F<sub>5</sub>)<sub>3</sub>. The molecular weights of copolymers are increased at higher ethylene pressures and lower concentrations of VTEoS; however, high molecular weights are seen under all conditions. M<sub>n</sub> values reach 138 kg/mol under 600 psig ethylene and 0.5 M of VTEoS (entry 9, Table 1). In the Pd-catalyzed copolymerizations, only one –Si(OR)<sub>3</sub> unit is incorporated per chain due to silane-induced chain transfer.<sup>20b,21</sup> In contrast, polymers reported here contain numerous –Si(OEt)<sub>3</sub> groups per chain. For example, there are ca. 26 –Si(OR)<sub>3</sub> units on average per chain for the copolymer in entry 2, Table 1. Mechanistic studies described below will show that  $\beta$ -silyl elimination does occur in these systems but seldom leads to chain transfer.

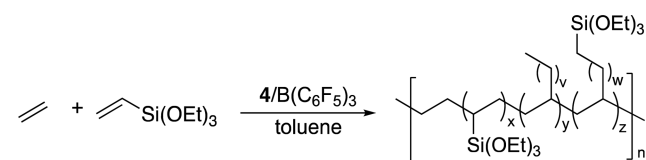
#### Investigation of Tetramethyl-Substituted Complex **4b**.

While highly branched copolymers are produced by tetraisopropyl-substituted catalyst **4a**, sparsely branched, nearly linear copolymers are generated using the less bulky tetramethyl-substituted complex **4b**.<sup>26</sup> Results are summarized in Table 3. Compared with **4a**/B(C<sub>6</sub>F<sub>5</sub>)<sub>3</sub>, **4b**/B(C<sub>6</sub>F<sub>5</sub>)<sub>3</sub> produces copolymers with higher VTEoS incorporation under similar reaction conditions and with similar TOFs. For example, compare entry 1, Table 3 (3.0 mol % incorporation, 4.1  $\times 10^4$  TOF) with entry 2, Table 1 (0.69 mol % incorporation, 5.3  $\times 10^4$  TOF). **4b**/B(C<sub>6</sub>F<sub>5</sub>)<sub>3</sub> also shows good thermal stability at 60 °C; the TOF for **4b**/B(C<sub>6</sub>F<sub>5</sub>)<sub>3</sub> is nearly constant over 60 min (entries 1 vs 2, Table 3). Like catalyst **4a**/B(C<sub>6</sub>F<sub>5</sub>)<sub>3</sub>, the incorporation of VTEoS is a

function of the ratio of VTEoS: ethylene (compare entry 1 to entry 3, and entry 5 to entry 6, Table 3) and the TOF is approximately proportional to ethylene pressure (entries 1 vs 6) and inversely proportional to VTEoS concentration (entries 1 vs 3 and 5 vs 6). An increase in temperature results in an increase in comonomer incorporation, and at 80 °C, 10 mol % VTEoS incorporation is achieved at 200 psig ethylene, 1.5 M silane (entry 4). As expected, the branching density decreases from 16 br/1000 C at 200 psig ethylene pressure to 9 br/1000 C at 600 psig ethylene (entries 1 vs 6). Notably, the TOF reaches 4.5  $\times 10^5$  h<sup>-1</sup>, under 600 psig ethylene, 0.1 M silane, 30 min, 60 °C, which is only ca. 4-fold lower than that of ethylene homopolymerization at 35 °C, with an incorporation ratio of 0.23 mol % (entries 7 vs 8, Table 3).

The microstructures of the copolymers obtained using catalyst **4b**/B(C<sub>6</sub>F<sub>5</sub>)<sub>3</sub> were analyzed by high temperature NMR spectroscopy to determine if the –Si(OEt)<sub>3</sub> groups were incorporated “in-chain” (on secondary carbons) or at chain ends (on primary carbons) (Scheme 2, see the SI for details). The mode of polar monomer incorporation is of particular interest as the reported ethylene-MA copolymers produced by  $\alpha$ -diimine Ni catalysts contain predominantly in-chain acrylate groups,<sup>15a,b</sup> which differs from copolymers of ethylene-MA generated with Pd  $\alpha$ -diimine catalysts where the functional group occurs at the ends of branches.<sup>4</sup> As noted previously, ethylene/

#### Scheme 2. In-Chain vs End-of-Chain Microstructures of Ethylene/VTEoS Copolymers

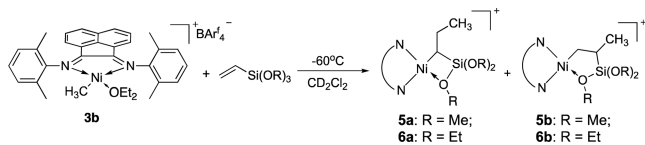


VTEoS copolymers produced with palladium  $\alpha$ -diimine catalysts are end-capped with  $-\text{Si}(\text{OR})_3$  due to silane-induced chain transfer. Table 3 summarizes the ratio of in-chain and chain-end silane incorporation (i.e.,  $x/z$ ) for polymers generated under various conditions (Scheme 2). Varying the concentration of VTEoS does not affect the ratio of in-chain to chain-end incorporation (entries 1 vs 3 and 5 vs 6, Table 3). However, the ratio is sensitive to the ethylene pressure and temperature. For example, the ratio decreases from 1.0:1.9 at 60 °C to 1.0:2.8 at 80 °C (entries 3 vs 4, Table 3) and increases from 1.0:1.9 at 200 psig ethylene to 1.0:1.1 at 600 psig ethylene (entries 3 vs 5, Table 3). A mechanistic rationalization of these results will be presented later in the paper.

**Mechanistic Studies.** Extensive low-temperature NMR spectroscopic investigations have been carried out in order to determine the structures and behavior of intermediates during chain growth and the nature of the catalyst resting state(s) and to elucidate the full details of the chain growth process.

**Chelate Formation: Reactions of ( $\alpha$ -Diimine)Ni(Me)(OEt)<sub>2</sub><sup>+</sup> 3b with Vinyltrialkoxysilanes.** Diethyl ether complex 3b was used for low-temperature studies since it has been previously established that the weakly bound diethyl ether ligand can be readily displaced at exceptionally low temperatures.<sup>22,24b</sup> In order to generate simplified NMR spectra, vinyltrimethoxysilane (VTMoS) was initially used in place of VTEoS. Addition of 2 equiv of VTMoS to a CD<sub>2</sub>Cl<sub>2</sub> solution of 3b at  $-80$  °C leads to slow insertion of the monomer without detectable formation of either the  $\kappa$ -O complex, ( $\alpha$ -diimine)Ni(Me)[( $\kappa$ -OMe)Si(OMe)<sub>2</sub>(C<sub>2</sub>H<sub>3</sub>)<sup>+</sup>], or the  $\eta^2$ -olefin complex (Scheme 3). The

**Scheme 3. Reactions of ( $\alpha$ -Diimine)Ni(Me)(OEt)<sub>2</sub><sup>+</sup> 3b with Vinyltrialkoxysilanes**



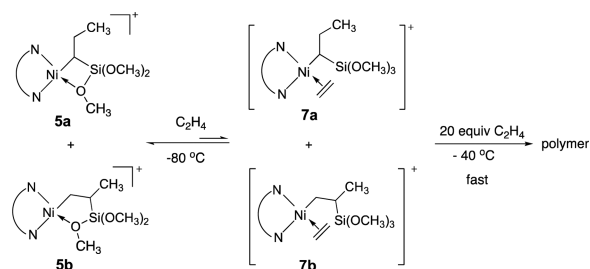
insertion is fast and complete at  $-60$  °C, yielding chelate complexes from both 2,1- and 1,2-insertions. The 2,1-insertion reaction generates four-membered chelate complex 5a and is favored over 1,2-insertion that forms five-membered chelate complex 5b by a ratio of 3:2. Both complexes exhibit fluxional behavior due to C–Si bond rotation and interchange of the coordinated  $-\text{OMe}$  groups ( $\delta = 3.81$  ppm for 5a, 2.86 ppm for 5b) with the two free  $-\text{OMe}$  groups, respectively. The rotational barriers for this process were measured via line-broadening techniques ( $\Delta G^\ddagger = \text{ca. } 10.5$  kcal/mol at  $-55$  °C for 5a,  $\Delta G^\ddagger = \text{ca. } 11.5$  kcal/mol at  $-45$  °C for 5b). Key <sup>1</sup>H NMR resonances for the static structure of complex 5a include signals at  $\delta$  0.79 ppm for the Ni-CH methine proton,  $\delta$  1.19 ppm and  $-0.22$  ppm for the methylene protons of NiCHCH<sub>2</sub>CH<sub>3</sub>, and  $\delta$  0.70 ppm for the methyl group of NiCHCH<sub>2</sub>CH<sub>3</sub>. Characteristic resonances of insertion product 5b include signals at  $\delta$  1.43 and 0.87 ppm for the diastereotopic methylene protons of Ni-CH<sub>2</sub>,  $\delta$   $-0.31$  ppm for the Si-CH methine proton and  $\delta$  1.17 ppm for the methyl group at C- $\beta$  of the chelate.

In addition to VTMoS, VTEoS was also investigated. Treatment of 3b with 2 equiv of VTEoS in CD<sub>2</sub>Cl<sub>2</sub> at  $-80$  °C results in slow diethyl ether displacement by olefin again with no observation of the intermediate  $\eta^2$ -olefin complex. Insertion at more convenient rates is observed at  $-60$  °C, yielding both 2,1-

insertion product 6a and 1,2-insertion product 6b in a ratio of 1:1. Dynamic behavior identical to the previous VTMoS case is observed, with the chelated and free ethoxy groups of both complexes distinguishable in the NMR spectrum at  $-80$  °C ( $\delta$  2.91 ppm for  $\kappa$ -OCHH'CH<sub>3</sub> and 2.78 ppm for  $\kappa$ -OCHH'CH<sub>3</sub> in complex 6a;  $\delta$  3.32 ppm for  $\kappa$ -OCHH'CH<sub>3</sub> and 3.22 ppm for  $\kappa$ -OCHH'CH<sub>3</sub> in complex 6b).

**Chelate Opening and Chain Propagation: Reactions of 5a,b with Ethylene.** The addition of excess ethylene to a mixture of 5a and 5b at  $-80$  °C in CD<sub>2</sub>Cl<sub>2</sub> results in much more rapid site exchange of the bound  $-\text{OMe}$  group with the two free  $-\text{OMe}$  groups as shown by NMR line-broadening experiments. Furthermore, the rate of site exchange increases with ethylene concentration.<sup>28</sup> This implies that, in the presence of ethylene, chelates rapidly open to form  $\eta^2$ -ethylene complexes, 7a and 7b, but that the equilibrium lies to the side of the chelates (Scheme 4). Upon warming solutions of 5a and 5b under 20 equiv of

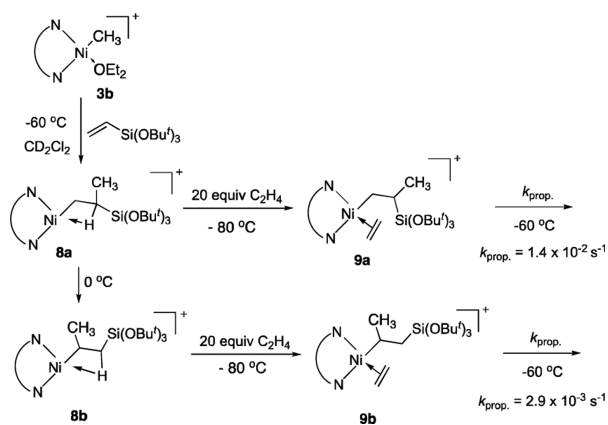
**Scheme 4. Chelate Opening by Ethylene and Chain Propagation**



ethylene to  $-40$  °C, rapid ethylene consumption is observed with formation of polymer, but with no concomitant significant decrease in concentration (less than 5%) of 5a and 5b. This behavior is due to slow initiation. Once 7a and 7b undergo insertion, chelate formation is disfavored and fast multiple insertions of ethylene ensue, so only a small fraction of 5a and 5b is consumed.<sup>29</sup>

In order to obtain the insertion rate from a “chelate-opened” ethylene complex, bulky vinyltri(*tert*-butoxy)silane (VTBoS) was evaluated (Scheme 5). Treatment of 3b with 2 equiv of VTBoS at  $-60$  °C leads to rapid insertion without detection of a  $\kappa$ -O complex ( $\alpha$ -diimine)Ni(Me)[( $\kappa$ -OBu<sup>t</sup>)Si(OBu<sup>t</sup>)<sub>2</sub>(C<sub>2</sub>H<sub>3</sub>)<sup>+</sup> or  $\eta^2$ -olefin-bound complex intermediates. The 1,2-insertion product is exclusively formed, which, surprisingly, is a stable agostic species 8a presumably due to the extreme steric bulk of

**Scheme 5. Chain Propagation of VTBoS via Complexes 9a,b**

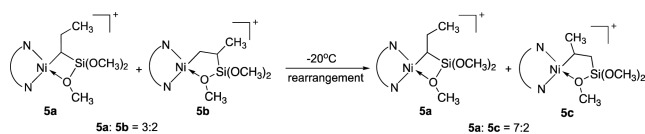


the *tert*-butoxy group which hinders chelate formation. Characteristic resonances of complex **8a** were observed at  $\delta$  1.54 and 1.44 ppm for the diastereotopic methylene protons of Ni-CH<sub>2</sub>,  $\delta$  -10.55 ppm for the agostic proton of C( $\mu$ -H)CH<sub>3</sub> and 1.28 ppm for the methyl protons of C( $\mu$ -H)CH<sub>3</sub>. Upon warming to 0 °C, complex **8a** slowly isomerized to the complex **8b**. Characteristic resonances of complex **8b** were observed at  $\delta$  1.75–1.77 ppm (m, NiCH(CH<sub>3</sub>)CH( $\mu$ -H)), -0.13 ppm (d, <sup>3</sup>J<sub>HH</sub> = 5.4 Hz, NiCH(CH<sub>3</sub>)CH( $\mu$ -H)), -0.86 ppm (dd, <sup>2</sup>J<sub>HH</sub> = 8.4 Hz and <sup>3</sup>J<sub>HH</sub> = 12.0 Hz, NiCH(CH<sub>3</sub>)CH( $\mu$ -H)), and -8.96 ppm (d, <sup>2</sup>J<sub>HH</sub> = 8.4 Hz, NiCH(CH<sub>3</sub>)CH( $\mu$ -H)). Addition of 20 equiv of ethylene to the CD<sub>2</sub>Cl<sub>2</sub> solution of complex **8a** at -80 °C leads to quantitative formation of a complex assigned as the ethylene-trapped complex **9a**, based on the disappearance of the agostic resonance and identification of bound ethylene resonances ( $\delta$  5.04, 4.54, 3.92, and 3.70 ppm, 1H each). For the complex **9a**, the turnover frequency ( $1.4 \times 10^{-2} \text{ s}^{-1}$ ) corresponding to the average rate of migratory insertion during chain growth was measured by the rate of decrease of signal for free ethylene in solution at -60 °C; the corresponding activation barrier,  $\Delta G^\ddagger$ , was determined to be 14.1 kcal/mol, which is nearly the same as that for the *n*-propyl ethylene nickel complex in ethylene homopolymerization.<sup>24b</sup> Similarly for complex **9b**, the turnover frequency was found to be  $2.9 \times 10^{-3} \text{ s}^{-1}$  ( $\Delta G^\ddagger = 14.8 \text{ kcal/mol}$ , -60 °C). This barrier is slightly higher than that of the complex **9a** and similar to that of the isopropyl ethylene nickel complex in ethylene homopolymerization.<sup>24b</sup> These activation barriers are nearly identical to ethylene homopolymerization barriers and suggest that the insertion barriers of chelate-opened ethylene complexes are not a factor in retarding the activity of copolymerizations.<sup>30</sup>

**Chelate Isomerization via  $\beta$ -Silyl Elimination.** As noted above, the copolymers produced using these nickel catalysts exhibit both in-chain and chain-end incorporation of -Si(OEt)<sub>3</sub>, and the ratio of these two modes of enchainment is affected by ethylene pressure and reaction temperature. Isomerizations of initially formed chelates likely play a role in determining in-chain vs chain-end incorporation of -Si(OEt)<sub>3</sub>. Thus, the isomerization behavior of the chelates was studied in the absence of ethylene.

Warming a mixture of chelates **5a** and **5b** to -20 °C results in a decrease and eventual disappearance of **5b** as complex **5c** grows in (Scheme 6). The initial ratio of **5a**:**5b** is ca. 3:2, while the final

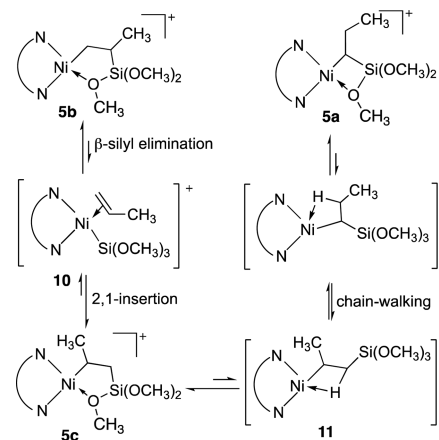
**Scheme 6. Isomerizations of Chelate Complexes 5a,b**



product ratio of **5a**:**5c** is ca. 7:2, which suggests that **5a** can be formed from both **5b** and **5c** and that the final ratio represents an equilibrium distribution of these three species. Characteristic resonances of chelate **5c** include signals at  $\delta$  1.48 ppm and -1.64 ppm for the diastereotopic methylene protons of Si-CH<sub>2</sub>,  $\delta$  1.67 ppm for the Ni-CH methine proton and  $\delta$  -0.10 ppm for the methyl group at C- $\alpha$  of the chelate.

The mechanism proposed for the isomerization of complex **5b** to complexes **5a** and **5c** is shown in Scheme 7. Opening of chelate complex **5b** followed by  $\beta$ -silyl elimination results in the formation of trimethoxysilyl  $\eta^2$ -propylene intermediate **10** (precedence for such an intermediate has been seen in the Pd

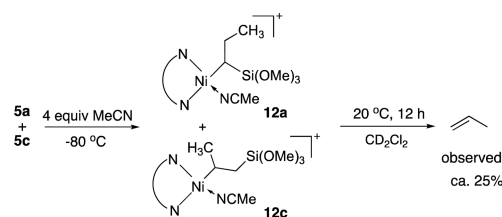
**Scheme 7. Proposed Mechanism of Chelate Isomerization**



system).<sup>20b</sup> 2,1-Migratory insertion of **10** forms complex **5c**. Subsequent “chain-walking” via intermediate **11** yields the complex **5a**.

If all steps are reversible, low concentrations of intermediate **10** could potentially be intercepted by an incoming ligand to generate free propylene (a major pathway in the Pd systems<sup>20b</sup>). Addition of 4 equiv of MeCN to the CD<sub>2</sub>Cl<sub>2</sub> solution of complexes **5a** and **5c** (7:2) at -80 °C results in rapid formation of chelate-opened MeCN complexes **12a** and **12c** in a 7:2 kinetic ratio (consistent with the starting 7:2 ratio of **5a**:**5c**) (Scheme 8).

**Scheme 8. Interception of Intermediate 10 with MeCN**



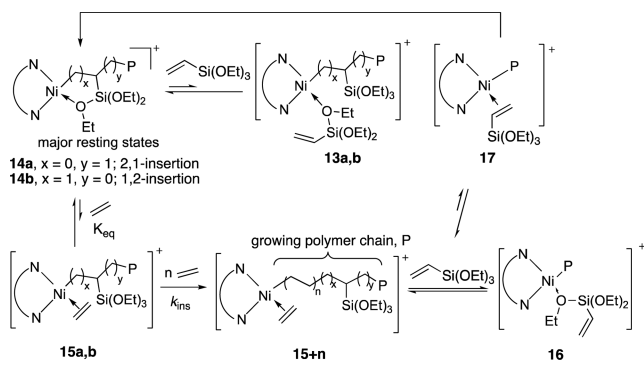
Warming the mixture of **12a** and **12c** at 20 °C over 12 h indeed results in observation of some free propylene (ca. 25%) which seems likely to result from interception of **10** formed via nitrile loss from **12a**, **12c** and isomerization as shown in Scheme 7.

## DISCUSSION

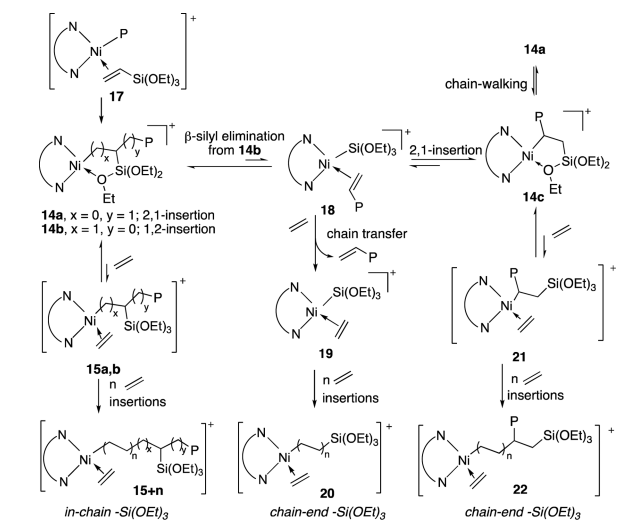
The mechanistic studies described above for the  $\alpha$ -diimine nickel catalysts yield a detailed picture of the chain-growth process and a rationale for the modes of enchainment of the VTEoS monomer as summarized below. Furthermore, these studies provide instructive comparisons with the quite different behavior of palladium  $\alpha$ -diimine systems for the analogous copolymerizations.

**Chain Growth.** The proposed general mechanism of chain growth in the nickel system is shown in Scheme 9. Refinement of this mechanism to account for chelate isomerization is discussed in the following section in conjunction with Scheme 10. Chelate complexes **14a,b** are the major catalyst resting states since mechanistic studies establish that the equilibria between **14a,b** and the ethylene complexes **15a,b**, favor **14a,b**, and in addition, the equilibria with ether-bound complexes **13a,b** also strongly favor **14a,b**.<sup>31</sup> Analyzing chain growth starting from resting states **14a,b**, the productive cycle involves reaction of these chelates with ethylene to form alkyl ethylene complexes **15a,b**, followed

## Scheme 9. Proposed Mechanism of Chain Growth



## Scheme 10. Proposed Mechanism of Modes of Silane Enchainment



by multiple insertions of ethylene to yield **15+n**, then coordination of VTEoS to yield **17** followed by insertion to return to resting states **14a,b**. We have established that the rate of the first ethylene insertion starting from **14a,b** will be proportional to  $k_{\text{ins}}K_{\text{eq}}[\text{C}_2\text{H}_4]$  and will be slower than subsequent insertions since the equilibria strongly favor **14a,b** (although we do not know the precise value of  $K_{\text{eq}}$ , see Scheme 4 and associated text). Judging from previous results for the Pd analogue,  $k_{\text{ins}}$  involving the initially opened chelate **15b** is likely very similar to known  $k_{\text{ins}}$  values for **15+n**. This contention is supported by results obtained here for the barriers to insertion of the tri-*tert*-butoxy systems **9a,b**. (While we have no models for insertion of **15a**, we know **14a** is in rapid equilibrium with **15a**

and that TOFs are constant over many minutes so **14a** is not an unreactive sink; otherwise, activity would soon cease. Furthermore, rearrangements of these chelates can occur so **14a** could rearrange to a more reactive chelate (see below). Multiple rapid ethylene insertions from **15a,b** occur through the primary species responsible for chain growth, **15+n**.<sup>32</sup> We established previously that homopolymerization of ethylene as well as these copolymerizations are retarded by  $\text{Si}(\text{OEt})_4$ , implying that VTEoS can compete with ethylene to remove quite significant concentrations of **15+n** from the cycle by forming unreactive ether complexes **16**, thus retarding the rate of chain growth. The binding affinity of VTEoS via a  $\pi$ -interaction is weaker than that of ethylene so the concentration of **17** will be low relative to **14a,b**, **15+n**, and **16**.

This mechanistic scenario is consistent with an effective TOF that is first-order in ethylene and inverse order in VTEoS and contrasts with the palladium system in which the ethylene complex is the resting state and the TOF is zero-order in ethylene. Despite the fact that the alkyl ethylene complexes responsible for chain growth are only a fraction of the species in solution, the Ni systems, due to lower ethylene insertion barriers, are much more active than the Pd systems<sup>20b</sup> (ca. 400-fold under similar conditions) in which the dominant resting state(s) are the alkyl ethylene complexes. The nickel catalysts show enhanced lifetimes in copolymerization relative to homopolymerization, and thus, higher productivities than expected are observed based on comparisons of initial TOFs. The enhanced catalyst lifetimes are likely a result of higher thermal stabilities of the chelate complexes **14a,b** relative to **15+n** and **16**.

**Chelate Isomerizations: In-Chain vs Chain-End -Si(OR)<sub>3</sub> Incorporation/Chain Transfer.** In Scheme 9, resting states **14a,b** were proposed on the basis of initial products of reaction of methyl ether complex **3b** with vinyltrialkoxysilanes to form **5a,b** and **6a,b**. From analysis of the copolymers formed from **4b** (Table 3), both in-chain and chain-end  $-\text{Si}(\text{OEt})_3$  groups are observed. Since insertion of ethylene into **14a,b** yields only in-chain  $-\text{Si}(\text{OEt})_3$  structures, the chain growth process must be more complex than shown in Scheme 9. As shown in Scheme 7, initially formed chelates can isomerize via  $\beta$ -Si(OMe)<sub>3</sub> elimination to form **5c** in which the  $-\text{Si}(\text{OMe})_3$  group is attached to a primary carbon. Thus, chain-end  $-\text{Si}(\text{OEt})_3$  groups can arise via the process shown in Scheme 10.  $\beta$ -Silyl elimination from **14b** produces the silyl complex **18**. Displacement of the unsaturated chain (chain transfer) in **18** by ethylene yields **19**, which would proceed on to give a  $-\text{CH}_2\text{CH}_2\text{Si}(\text{OEt})_3$  end-functionalized polymer.<sup>33</sup> This is the dominant pathway in the Pd systems<sup>20b</sup> but can only be a minor pathway here since there are many  $-\text{CH}_2\text{Si}(\text{OEt})_3$  groups per chain.<sup>34</sup> From **18**, 2,1-insertion yields chelate **14c** (analogous to **5c**, Scheme 7).

Table 4. Copolymerization of Ethylene and VTEoS Using ( $\alpha$ -Diimine)NiBr<sub>2</sub> **2**<sup>a</sup>

entry	precatalyst	C <sub>2</sub> H <sub>4</sub> (psig)	time (h)	TOF ( $\times 10^{-4} \text{ h}^{-1}$ )	productivity (kg copolymer/g Ni)	branches/ 1000 C <sup>b</sup>	M <sub>n</sub> <sup>c</sup> (kg/mol)	M <sub>w</sub> / M <sub>n</sub> <sup>c</sup>	incorp <sup>b</sup> (mol %)	T <sub>m</sub> <sup>d</sup> (°C)
1	<b>2a</b>	200	0.5	12.9	29	54	112	1.8	0.60	66
2	<b>2a</b>	200	1.0	11.0	53	54	114	1.8	0.60	65
3	<b>2b</b>	600	0.5	23.6	58	9	39	1.4	0.84	113
4 <sup>e</sup>	<b>2b</b>	600	0.5	44.3	106	10	35	1.6	0.41	115
5 <sup>e,f</sup>	<b>2b</b>	600	1.5	38.1	275	10	35	1.6	0.43	116
6 <sup>f,g</sup>	<b>2b</b>	600	4.0	29.0	560	11	33	1.9	0.23	115

<sup>a</sup>V(total) = 50 mL, 1.5  $\mu\text{mol}$  of **2**, [0.5 M] VTEoS, 60 °C, 15  $\mu\text{mol}$  B(C<sub>6</sub>F<sub>5</sub>)<sub>3</sub>, 0.3 mmol of AlMe<sub>3</sub>, 15  $\mu\text{mol}$  of [Ph<sub>3</sub>C][B(C<sub>6</sub>F<sub>5</sub>)<sub>4</sub>], toluene solvent.  
<sup>b</sup>Determined by using <sup>1</sup>H NMR spectroscopy. <sup>c</sup>M<sub>n</sub> and M<sub>w</sub>/M<sub>n</sub> were determined by SEC in trichlorobenzene at 150 °C. <sup>d</sup>Determined by differential scanning calorimetry, second heating. <sup>e</sup>V(total) = 200 mL. [0.2 M] VTEoS. <sup>f</sup>0.6 mmol of AlMe<sub>3</sub>. <sup>g</sup>V(total) = 400 mL. [0.1 M] VTEoS.

Trapping by ethylene and insertion yields **22** resulting in chain-end incorporation of silane.<sup>35</sup> This pathway is likely the dominant pathway for chain-end  $-\text{Si}(\text{OEt})_3$  incorporation.

This scheme is consistent with the dependence of the in-chain to chain-end ratios on temperature and ethylene pressure as shown in Table 3. As ethylene pressure is increased, one would expect faster trapping of chelates **14a,b** and insertion to yield in-chain silane relative to chelate isomerization to **18/14c** and formation of chain-end silanes. This trend is verified in comparing entry 1 (200 psig ethylene) with entry 6 (600 psig ethylene) where chain-end silanes decrease substantially (1.9:1.0 vs 1.1:1.0). Similarly, the rate of chelate isomerization (first-order process) relative to trapping (second-order process) should increase with temperature. Indeed comparing entry 3 (60 °C) with entry 4 (80 °C) shows such a trend (1.9:1.0 vs 2.8:1.0). Since copolymers exhibit 50% or greater chain-end incorporated silane, we must conclude that species **14c** plays a significant role in chain growth. From this data, we cannot say whether **14c** is a significant resting state or whether conversion of **14c** to **22** is simply faster than conversion of **14a,b** to **15+n** and thus never builds up in significant concentrations.

**Convenient Synthesis of Vinyltriethoxysilane/Ethylene Copolymers.** Finally, a highly active and productive catalyst system has been devised via activation of easily synthesized and air-stable ( $\alpha$ -diimine) $\text{NiBr}_2$  complexes **2a,b**.<sup>36</sup> Selected copolymerization results are summarized in Table 4 using **2a,b** activated by a combination of commercially available activators  $\text{AlMe}_3$ ,  $\text{B}(\text{C}_6\text{F}_5)_3$  and  $[\text{Ph}_3\text{C}][\text{B}(\text{C}_6\text{F}_5)_4]$  (see Table S2 for details). Cross-linking of isolated copolymers does not occur under these conditions as is common using other activation procedures.<sup>20a</sup> Compared with ( $\alpha$ -diimine) $\text{Ni}(\text{Me})(\text{CH}_3\text{CN})^+$  complexes **4**, this catalyst system produces similar copolymers but with a higher (ca. 2-fold) activity (compare entry 2, Table 1 vs entry 1, Table 4 and entry 6, Table 3 vs entry 3, Table 4). The productivity of the system is found to be ca. 2 times higher than the DuPont system with a similar VTEoS incorporation (ca. 0.4 mol %) under similar conditions (eq 1 vs entry 5). Furthermore, the productivity reaches 275 kg copolymer/g Ni in 1.5 h with 0.43 mol % silane incorporation (entry 5) and 560 kg copolymer/g Ni in 4 h with 0.23 mol % silane incorporation (entry 6). Since only low levels of  $-\text{Si}(\text{OEt})_3$  are needed for cross-linking these results suggest possible commercial potential for production of cross-linkable PE using this method. Experiments demonstrating that these copolymers can be cross-linked have been added to the SI.<sup>37</sup>

## SUMMARY

Comprehensive synthetic and mechanistic studies of the  $\alpha$ -diimine nickel-catalyzed copolymerizations of ethylene and vinyltrialkoxysilanes, including low-temperature NMR studies of intermediates, provide a complete description of the chain growth process that differs in numerous crucial details with respect to the analogous palladium chemistry. Key findings are summarized below:

The cationic  $\alpha$ -diimine Ni complexes **4a,b**/ $\text{B}(\text{C}_6\text{F}_5)_3$  catalyze copolymerization of ethylene and VTEoS at 60 °C to give nearly linear to highly branched high  $M_n$  copolymer depending on catalyst choice and reaction conditions with high turnover frequencies (up to  $4.5 \times 10^3 \text{ h}^{-1}$ ), good lifetimes, and high overall productivity. Incorporation levels of VTEoS range from 0.23 to 10.0 mol % with multiple  $-\text{Si}(\text{OEt})_3$  groups incorporated per chain. In contrast, palladium analogs produce low  $M_n$  polymers/oligomers with modest overall productivities due to low TOFs,

reduced catalyst lifetimes and a single  $-\text{Si}(\text{OEt})_3$  group incorporated at the chain end.<sup>20b</sup>

Low temperature NMR studies show that the vinyltrialkoxysilanes insert into Ni–R bonds in both 2,1- and 1,2-modes to yield 4- and 5-membered chelates involving coordination of the Si–O–R moiety to the Ni center. These chelates are the catalyst resting states and account for a TOF that is first-order in ethylene and inverse-order in silane. The chelates react rapidly with ethylene to yield “opened” ethylene alkyl complexes but the chelates are energetically favored. In contrast, the resting state(s) of the Pd systems are alkyl olefin complexes and the TOF is independent of silane concentration and ethylene pressure.

The ratio of in-chain/chain-end incorporation of  $-\text{Si}(\text{OR})_3$  groups increases with ethylene pressure and decreases with an increase in temperature. Low-temperature NMR studies show that chain-end incorporation of  $-\text{Si}(\text{OR})_3$  groups arises from chelate rearrangement via a  $\beta$ -silyl elimination mechanism. In the Pd analogues,  $\beta$ -silyl elimination accounts for the primary chain transfer mechanism resulting in low  $M_n$  polymers with incorporation of only one  $-\text{Si}(\text{OR})_3$  group per chain. Such chain transfer events are rare in the Ni systems.

Polyethylene functionalized with  $-\text{Si}(\text{OR})_3$  groups is a commercial polymer used to prepare PEX-b via cross-linking of the  $-\text{Si}(\text{OR})_3$  groups by exposure to moisture.  $\text{Si}(\text{OR})_3$ -functionalized PE is prepared commercially by grafting vinyl silanes onto PE or via radical-initiated copolymerization of ethylene and a vinyl silane under high pressures and temperatures. We have developed here a convenient Ni-catalyzed copolymerization route using as precatalysts easily accessible  $\alpha$ -diimine nickel dibromides in combination with commercial activators,  $\text{AlMe}_3/\text{B}(\text{C}_6\text{F}_5)_3/[\text{Ph}_3\text{C}][\text{B}(\text{C}_6\text{F}_5)_4]$ . Excellent activities and productivities using this catalyst system can be obtained. For example, copolymers containing 0.23 mol % triethoxysilane groups can be generated at 60 °C, 600 psig ethylene over 4 h with a productivity of 560 kg of copolymer/g Ni.

## ASSOCIATED CONTENT

### Supporting Information

The Supporting Information is available free of charge on the ACS Publications website at DOI: 10.1021/jacs.7b10281.

Detailed experimental procedures, characterization data for complexes **4a,b**, **5a–c**, **6a,b**, **8a,b**, **9a,b**, and **12a,c**, NMR spectra of copolymers, kinetic plots, and cross-linking experiments (PDF)

## AUTHOR INFORMATION

### Corresponding Authors

\*E-mail: mbrookhart@unc.edu.

\*E-mail: olafs@uh.edu.

### ORCID

Zhou Chen: 0000-0003-4345-7070

Olafs Daugulis: 0000-0003-2642-2992

### Notes

The authors declare the following competing financial interest(s): The authors have submitted a provisional patent on portions of this work.

## ACKNOWLEDGMENTS

This research was supported by the National Science Foundation (CHE-1010170 to M.B.), DuPont, and the Welch Foundation (Chair E-0044 to O.D. and Grant E-1893 to M.B.).

## REFERENCES

- (1) (a) Boardman, B. M.; Bazan, G. C. *Acc. Chem. Res.* **2009**, *42*, 1597–1606. (b) Wan, D.-W.; Gao, Y.-S.; Li, J.-F.; Shen, Q.; Sun, X.-L.; Tang, Y. *Dalton Trans.* **2012**, *41*, 4552–4557. (c) Baier, M. C.; Zuideveld, M. A.; Mecking, S. *Angew. Chem., Int. Ed.* **2014**, *53*, 9722–9744. (d) Mu, H.; Pan, L.; Song, D.; Li, Y. *Chem. Rev.* **2015**, *115*, 12091–12137. (e) Small, B. L. *Acc. Chem. Res.* **2015**, *48*, 2599–2611. (f) Guo, L.; Dai, S.; Sui, X.; Chen, C. *ACS Catal.* **2016**, *6*, 428–441.
- (2) (a) Ittel, S. D.; Johnson, L. K.; Brookhart, M. *Chem. Rev.* **2000**, *100*, 1169–1203. (b) Boffa, L. S.; Novak, B. M. *Chem. Rev.* **2000**, *100*, 1479–1493. (c) Luo, S.; Jordan, R. F. *J. Am. Chem. Soc.* **2006**, *128*, 12072–12073. (d) Dong, J.-Y.; Hu, Y. *Coord. Chem. Rev.* **2006**, *250*, 47–65. (e) Berkefeld, A.; Mecking, S. *Angew. Chem., Int. Ed.* **2008**, *47*, 2538–2542. (f) Nakamura, A.; Ito, S.; Nozaki, K. *Chem. Rev.* **2009**, *109*, 5215–5244. (g) Chen, C.; Luo, S.; Jordan, R. F. *J. Am. Chem. Soc.* **2010**, *132*, 5273–5284.
- (3) Johnson, L. K.; Mecking, S.; Brookhart, M. *J. Am. Chem. Soc.* **1996**, *118*, 267–268.
- (4) Mecking, S.; Johnson, L. K.; Wang, L.; Brookhart, M. *J. Am. Chem. Soc.* **1998**, *120*, 888–899.
- (5) Nakamura, A.; Anselment, T. M. J.; Claverie, J.; Goodall, B.; Jordan, R. F.; Mecking, S.; Rieger, B.; Sen, A.; van Leeuwen, P. W. N. M.; Nozaki, K. *Acc. Chem. Res.* **2013**, *46*, 1438–1449.
- (6) (a) Carrow, B. P.; Nozaki, K. *J. Am. Chem. Soc.* **2012**, *134*, 8802–8805. (b) Contrella, N. D.; Sampson, J. R.; Jordan, R. F. *Organometallics* **2014**, *33*, 3546–3555. (c) Zhang, Y.; Cao, Y.; Leng, X.; Chen, C.; Huang, Z. *Organometallics* **2014**, *33*, 3738–3745. (d) Sui, X.; Dai, S.; Chen, C. *ACS Catal.* **2015**, *5*, 5932–5937. (e) Carrow, B. P.; Zhang, W. *WO 2015200849*, 2015.
- (7) (a) Drent, E.; van Dijk, R.; van Ginkel, R.; van Oort, B.; Pugh, R. I. *Chem. Commun.* **2002**, 744–745. (b) Kochi, T.; Yoshimura, K.; Nozaki, K. *Dalton Trans.* **2006**, 25–27. (c) Skupov, K. M.; Marella, P. R.; Simard, M.; Yap, G. P. A.; Allen, N.; Conner, D.; Goodall, B. L.; Claverie, J. P. *Macromol. Rapid Commun.* **2007**, *28*, 2033–2038. (d) Guironnet, D.; Roesle, P.; Rünzi, T.; Göttker-Schnetmann, I.; Mecking, S. *J. Am. Chem. Soc.* **2009**, *131*, 422–423.
- (8) Ito, S.; Munakata, K.; Nakamura, A.; Nozaki, K. *J. Am. Chem. Soc.* **2009**, *131*, 14606–14607.
- (9) (a) Weng, W.; Shen, Z.; Jordan, R. F. *J. Am. Chem. Soc.* **2007**, *129*, 15450–15451. (b) Wada, S.; Jordan, R. F. *Angew. Chem., Int. Ed.* **2017**, *56*, 1820–1824.
- (10) Kochi, T.; Noda, S.; Yoshimura, K.; Nozaki, K. *J. Am. Chem. Soc.* **2007**, *129*, 8948–8949.
- (11) Luo, S.; Vela, J.; Lief, G. R.; Jordan, R. F. *J. Am. Chem. Soc.* **2007**, *129*, 8946–8947.
- (12) (a) Skupov, K. M.; Piche, L.; Claverie, J. P. *Macromolecules* **2008**, *41*, 2309–2310. (b) Borkar, S.; Newsham, D. K.; Sen, A. *Organometallics* **2008**, *27*, 3331–3334. (c) Rünzi, T.; Fröhlich, D.; Mecking, S. *J. Am. Chem. Soc.* **2010**, *132*, 17690–17691. (d) Bouilhac, C.; Rünzi, T.; Mecking, S. *Macromolecules* **2010**, *43*, 3589–3590. (e) Ito, S.; Kanazawa, M.; Munakata, K.; Kuroda, J.-i.; Okumura, Y.; Nozaki, K. *J. Am. Chem. Soc.* **2011**, *133*, 1232–1235. (f) Friedberger, T.; Wucher, P.; Mecking, S. *J. Am. Chem. Soc.* **2012**, *134*, 1010–1018. (g) Jian, Z.; Baier, M. C.; Mecking, S. *J. Am. Chem. Soc.* **2015**, *137*, 2836–2839.
- (13) (a) Johnson, L. K.; Killian, C. M.; Brookhart, M. *J. Am. Chem. Soc.* **1995**, *117*, 6414–6415. (b) Camacho, D. H.; Salo, E. V.; Ziller, J. W.; Guan, Z. *Angew. Chem., Int. Ed.* **2004**, *43*, 1821–1825. (c) Cherian, A. E.; Rose, J. M.; Lobkovsky, E. B.; Coates, G. W. *J. Am. Chem. Soc.* **2005**, *127*, 13770–13771. (d) Meinhard, D.; Wegner, M.; Kipiani, G.; Hearley, A.; Reuter, P.; Fischer, S.; Marti, O.; Rieger, B. *J. Am. Chem. Soc.* **2007**, *129*, 9182–9191. (e) Liu, F.-S.; Hu, H.-B.; Xu, Y.; Guo, L.-H.; Zai, S.-B.; Song, K.-M.; Gao, H.-Y.; Zhang, L.; Zhu, F.-M.; Wu, Q. *Macromolecules* **2009**, *42*, 7789–7796. (f) Rhinehart, J. L.; Brown, L. A.; Long, B. K. *J. Am. Chem. Soc.* **2013**, *135*, 16316–16319. (g) Zhang, D.; Nadres, E. T.; Brookhart, M.; Daugulis, O. *Organometallics* **2013**, *32*, 5136–5143.
- (14) (a) Zhou, X.; Bontemps, S.; Jordan, R. F. *Organometallics* **2008**, *27*, 4821–4824. (b) Guironnet, D.; Rünzi, T.; Göttker-Schnetmann, I.; Mecking, S. *Chem. Commun.* **2008**, 4965–4967. (c) Noda, S.; Kochi, T.; Nozaki, K. *Organometallics* **2009**, *28*, 656–658. (d) Perrotin, P.; McCahill, J. S. J.; Wu, G.; Scott, S. L. *Chem. Commun.* **2011**, *47*, 6948–6950. (e) Wu, Z.; Chen, M.; Chen, C. *Organometallics* **2016**, *35*, 1472–1479.
- (15) (a) Johnson, L.; Bennett, A.; Dobbs, K.; Hauptman, E.; Ionkin, A.; Ittel, S.; McCord, E.; McLain, S.; Radzewich, C.; Yin, Z.; Wang, L.; Wang, Y.; Brookhart, M. *Polym. Mater. Sci. Eng.* **2002**, *86*, 319. (b) McLain, S.; Sweetman, K.; Johnson, L.; McCord, E. *Polym. Mater. Sci. Eng.* **2002**, *86*, 320. (c) Williams, B. S.; Leatherman, M. D.; White, P. S.; Brookhart, M. *J. Am. Chem. Soc.* **2005**, *127*, 5132–5146. (d) Long, B. K.; Eagan, J. M.; Mulzer, M.; Coates, G. W. *Angew. Chem., Int. Ed.* **2016**, *55*, 7106–7110. (e) Li, M.; Wang, X.; Luo, Y.; Chen, C. *Angew. Chem., Int. Ed.* **2017**, *56*, 11604–11609.
- (16) (a) Ito, S.; Ota, Y.; Nozaki, K. *Dalton Trans.* **2012**, *41*, 13807–13809. (b) Chen, M.; Chen, C. *ACS Catal.* **2017**, *7*, 1308–1312.
- (17) For other nickel systems, see: (a) Younkin, T. R.; Connor, E. F.; Henderson, J. I.; Friedrich, S. K.; Grubbs, R. H.; Bansleben, D. A. *Science* **2000**, *287*, 460–462. (b) Diamanti, S. J.; Ghosh, P.; Shimizu, F.; Bazan, G. C. *Macromolecules* **2003**, *36*, 9731–9735. (c) Berkefeld, A.; Drexler, M.; Möller, H. M.; Mecking, S. *J. Am. Chem. Soc.* **2009**, *131*, 12613–12622. (d) Radlauer, M. R.; Buckley, A. K.; Henling, L. M.; Agapie, T. *J. Am. Chem. Soc.* **2013**, *135*, 3784–3787. (e) Tao, W.-j.; Nakano, R.; Ito, S.; Nozaki, K. *Angew. Chem., Int. Ed.* **2016**, *55*, 2835–2839. (f) Leicht, H.; Göttker-Schnetmann, I.; Mecking, S. *ACS Macro Lett.* **2016**, *5*, 777–780. (g) Xin, B. S.; Sato, N.; Tanna, A.; Oishi, Y.; Konishi, Y.; Shimizu, F. *J. Am. Chem. Soc.* **2017**, *139*, 3611–3614.
- (18) (a) Tsunaga, M.; Matsunami, S.; Sato, M.; Nakata, K. *Plast., Rubber Compos.* **1998**, *27*, 460–464. (b) Rizzuto, P.; Baione, F.; Guerra, G.; Martinotto, L.; Albizzati, E. *Macromolecules* **2001**, *34*, 5175–5179. (c) Khonakdar, H. A.; Morshedian, J.; Wagenknecht, U.; Jafari, S. H. *Polymer* **2003**, *44*, 4301–4309.
- (19) (a) Narkis, M.; Tzur, A.; Vaxman, A.; Fritz, H. G. *Polym. Eng. Sci.* **1985**, *25*, 857–862. (b) Celina, M.; George, G. A. *Polym. Degrad. Stab.* **1995**, *48*, 297–312.
- (20) (a) Johnson, L. K.; McLain, S. J.; Sweetman, K. J.; Wang, Y.; Bennett, A. M. A.; Wang, L.; McCord, E. F.; Lonkin, A.; Ittel, S. D.; Radzewich, C. E.; Schifano, R. S. *WO 2003044066*, 2003. (b) Chen, Z.; Liu, W.; Daugulis, O.; Brookhart, M. *J. Am. Chem. Soc.* **2016**, *138*, 16120–16129.
- (21) Sandwich  $\alpha$ -diimine Pd(II) catalysts exhibit enhanced axial bulk such that chain transfer via  $\beta$ -silyl elimination is inhibited and high  $M_w$  copolymers are obtained using these catalysts.
- (22) Svejda, S. A.; Johnson, L. K.; Brookhart, M. *J. Am. Chem. Soc.* **1999**, *121*, 10634–10635.
- (23) For a reported MeCN complex for ethylene polymerization, see: Daugulis, O.; Brookhart, M.; White, P. S. *Organometallics* **2003**, *22*, 4699–4704.
- (24) (a) Shultz, L. H.; Tempel, D. J.; Brookhart, M. *J. Am. Chem. Soc.* **2001**, *123*, 11539–11555. (b) Leatherman, M. D.; Svejda, S. A.; Johnson, L. K.; Brookhart, M. *J. Am. Chem. Soc.* **2003**, *125*, 3068–3081.
- (25) Based on observations in the Pd system (ref 20b) the  $E_a$  for insertion of the vinyl silane is likely slightly higher than  $E_a$  for ethylene insertion. This could also partially account for the increasing incorporation of silane with increasing temperature.
- (26) Gates, D. P.; Svejda, S. A.; Oñate, E.; Killian, C. M.; Johnson, L. K.; White, P. S.; Brookhart, M. *Macromolecules* **2000**, *33*, 2320–2334.
- (27) An exception is the tetrabenzyl-substituted catalysts reported by Long (ref 13f).
- (28) A quantitative dynamic NMR line broadening study of chelate **5a** shows line-broadening of the bound  $-\text{OCH}_3$  resonance to be directly proportional to ethylene concentration at  $-80^\circ\text{C}$ . Exchange rates and concentrations were observed:  $84\text{ s}^{-1}$ ,  $0.0050\text{ M C}_2\text{H}_4$ ;  $181\text{ s}^{-1}$ ,  $0.0096\text{ M C}_2\text{H}_4$ ;  $287\text{ s}^{-1}$ ,  $0.014\text{ M C}_2\text{H}_4$ . These results show clearly that chelate **5a** is in rapid equilibrium with ethylene complex **7a** prior to insertion.
- (29) A polyethylene would be produced with a terminal  $-\text{Si}(\text{OMe})_3$  group, but its concentration is too low to be detected.
- (30) As noted, the rate constants measured are an average over multiple insertions. Due to overlap of signals **9a**, **9b** with subsequent ethylene complexes it was not possible to precisely measure “first insertion” barriers of **9a**, **9b**. However, we describe in the SI experiments

that suggest these barriers are slightly but not significantly higher than subsequent insertion barriers.

(31) This was established by treating **5a,b** with 0.05 M Si(OMe)<sub>4</sub> and observing that no adduct was formed in measurable concentrations.

(32) As established previously (ref 24), in homopolymerizations of ethylene using these nickel  $\alpha$ -diimine catalysts,  $\beta$ -agostic alkyl species will form as intermediates in chain propagation via successive ethylene insertions of **15+n**. The concentrations of these agostic species relative to ethylene complexes **15+n** will be low, since under these conditions, homopolymerizations are zero-order in ethylene and the resting state(s) are the ethylene alkyl complexes. However, even if the  $\beta$ -agostic species were present in significant amounts relative to the alkyl ethylene species, this would have no effect on the general mechanistic/kinetic analysis presented here.

(33) A reviewer has suggested that  $-\text{CH}_2\text{CH}_2\text{Si}(\text{OEt})_3$  polymer end groups could arise not only via  $\beta$ -silyl elimination, chain transfer, and ethylene insertion into Ni–Si(OEt)<sub>3</sub> but also via vinyl silane insertion into a Ni–H bond generated from  $\beta$ -H elimination. While vinyl silane competes poorly with ethylene for insertion into a Ni–R bond, it may compete well for insertion into the less bulky Ni–H group as demonstrated in other systems (refs 7–12). NMR analysis of the copolymers does not allow us to distinguish between these possibilities.

(34) This chain-transfer process is dominant in the Pd system (ref 20b) resulting in low  $M_n$  polymer/oligomers. Since high polymers are generated in the Ni systems, the rate of chain-transfer via this process relative to chain propagation must be small. Homopolymers generated have somewhat higher  $M_n$  values relative to copolymers generated under similar conditions. It seems plausible, since traces of propylene are observed on decay of **12a,b**, that  $M_n$  values are reduced via a minor  $\beta$ -silyl elimination chain-transfer pathway.

(35) Chain-walking from species **14c** and trapping could yield a complex of the type ( $\alpha$ -diimine)(ethylene)NiCHPCH<sub>2</sub>CH<sub>2</sub>Si(OEt)<sub>3</sub><sup>+</sup>. Insertion would then yield a copolymer exhibiting a PCH(CH<sub>2</sub>CH<sub>2</sub>Si(OEt)<sub>3</sub>)CH<sub>2</sub>CH<sub>2</sub>P' microstructural feature, with silane separated from the main chain by two methylene units. This possibility draws support from a preliminary observation that trapping **5a/5c** with Me<sub>2</sub>S yields the expected two products at  $-60$  °C which upon warming to  $-20$  °C yields an additional product, ( $\alpha$ -diimine)(SMe<sub>2</sub>)NiCH<sub>2</sub>CH<sub>2</sub>CH<sub>2</sub>Si(OMe)<sub>3</sub><sup>+</sup>.

(36) Svejda, S. A.; Brookhart, M. *Organometallics* **1999**, *18*, 65–74.

(37) Copolymers with the  $M_n$  of 30–40 kg/mol and  $M_w$  of 60–80 kg/mol should surely be sufficient to provide a tough cross-linked polymer. For a reported example, see: Zhang, G.; Wang, G.; Zhang, J.; Wei, P.; Jiang, P. *J. Appl. Polym. Sci.* **2006**, *102*, 5057–5061. Experiments showing generation of highly cross-linked insoluble material with high gel content are described in the SI.